AAPS PharmSciTech, Vol. 10, No. 2, June 2009 (© 2009)
DOI: 10.1208/s12249-009-9222-5

Research Article

Intratumoral Delivery of Paclitaxel in Solid Tumor from Biodegradable Hyaluronan Nanoparticle Formulations

Abeer M. Al-Ghananeem,[1,4] Ahmad H. Malkawi,[1] Yahya M. Muammer,[1] Justin M. Balko,[1] Esther P. Black,[1] Walid Mourad,[2] and Edward Romond[3]

Received 29 October 2008; accepted 9 March 2009; published online 21 April 2009

Abstract. In the current study, novel paclitaxel-loaded cross-linked hyaluronan nanoparticles were engineered for the local delivery of paclitaxel as a prototype drug for cancer therapy. The nanoparticles were prepared using a desolvation method with polymer cross-linking. *In vitro* cytotoxicity studies demonstrated that less than 75% of the MDA-MB-231 and ZR-75-1 breast cancer cells were viable after 2-day exposure to paclitaxel-loaded hyaluronan nanoparticles or free paclitaxel, regardless of the dose. These results suggest that hyaluronan nanoparticles maintain the pharmacological activity of paclitaxel and efficiently deliver it to the cells. Furthermore, *in vivo* administration of the drug-loaded nanoparticles via direct intratumoral injection to 7,12-dimethylbenz[a]anthracene (DMBA)-induced mammary tumor in female rats was studied. The paclitaxel-loaded nanoparticles treated group showed effective inhibition of tumor growth in all treated rats. Interestingly, there was one case of complete remission of tumor nodule and two cases of persistent reduction of tumor size that was observed on subsequent days. In the case of free paclitaxel-treated group, the mean tumor volume increased almost linearly (R^2=0.93) with time to a size that was 4.9-fold larger than the baseline volume at 57 days post-drug administration. Intratumoral administration of paclitaxel-loaded hyaluronan nanoparticles could be a promising treatment modality for solid mammary tumors.

KEY WORDS: hyaluronic acid; intratumor; mammary tumor; nanoparticles; paclitaxel.

INTRODUCTION

Many common solid tumors including breast, brain, and prostate tumors do not respond well to conventional systemic chemotherapy. An alternative approach to systemic administration of drugs for the treatment of localized tumor could be through loco-regional administration. This can be achieved by intra-arterial infusion of the chemotherapeutic agents upstream of the tumor and also through direct intratumor injection (1–3).

Microencapsulation of drugs using biodegradable polymers, delivered locally, provides a novel modality to increase therapeutic concentrations of a drug for a prolonged period while decreasing the drug systemic levels and the side effects. For localized delivery, paclitaxel has been formulated in biodegradable polymeric microspheres, nanoparticles, surgical pastes, and implants (4–6).

The attractive polysaccharide hyaluronic acid (HA; Fig. 1a) has been successfully used for several biomedical applications with the cytotoxic agent paclitaxel such as; macromolecular drug copolymer conjugate, hydrophilic coating, and hydrogels (7–10), but not as nanoparticle polymer system. HA is one of the main components of the extracellular matrix in the body. Since HA is a naturally occurring biopolymer, it is biocompatible and biodegradable. Furthermore, most malignant solid tumors and their surrounding stromal tissue contain elevated levels of HA (9). CD44 is the principal cell surface receptor for HA, and it presents at low levels on epithelial, hemopoietic and some neuronal cells (11–13), and at elevated levels in various carcinoma, lymphoma, breast, colorectal, and lung tumor cells (14–17). Overexpression of the HA receptors CD44 and RHAMM on cancer cells results in enhanced binding and endocytosis uptake of such compound.

Paclitaxel (PXL), the first taxane in clinical trials, is an active chemotherapeutic drug against a broad range of cancers, especially breast and ovarian cancers. PXL has shown a high potential as an anticancer drug, but its practical use is limited due to its low solubility in water as well as other pharmaceutical solvents compatible with intravenous administration. Paclitaxel is currently available as a solution in a vehicle composed of Cremophor® EL and dehydrated alcohol (Taxol®), or as an injectable suspension of albumin-bound paclitaxel nanoparticles (Abraxane®). However, these two commercial formulations had reported side effects

[1] Department of Pharmaceutical Sciences, College of Pharmacy, University of Kentucky, 927 Rose Street, Lexington, Kentucky 40536-0082, USA.
[2] Department of Pathology and Laboratory Medicine, College of Medicine, University of Kentucky, Lexington, Kentucky 40536, USA.
[3] Division of Hematology and Oncology, Markey Cancer Center, University of Kentucky, Lexington, Kentucky 40536, USA.
[4] To whom correspondence should be addressed. (e-mail: amalg0@email.uky.edu)

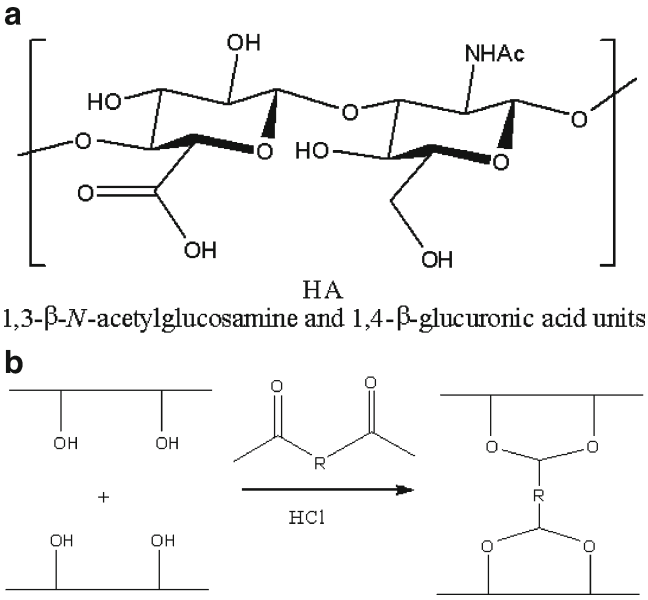

Fig. 1. **a** Structure of hyaluronic acid (HA) polysaccharide which is glycosaminoglycan copolymer of D-glucuronic acid and *N*-acetyl-D-glucosamine. **b** Chemical cross-linking of hyaluronic acid using glutaraldehyde

(18,19). Thus, safe and effective drug delivery systems are still in need to improve the current clinical chemotherapeutic treatments with PXL.

To our knowledge, there are no examples of HA nanoparticles as a delivery system for chemotherapeutic agents. Therefore, taking into account the favorable biological and physicochemical properties of HA, it is reasonable to hypothesize that HA nanoparticles could improve paclitaxel cytotoxicity to tumor cells. In the current study, novel paclitaxel-loaded cross-linked hyaluronan nanoparticles (PXL-HA NPs) were engineered for the local delivery of paclitaxel (PXL) as a prototype drug for cancer therapy. Furthermore, the drug-loaded nanoparticles efficacy was tested through direct intratumoral administration to 7,12-dimethylbenz[a]anthracene (DMBA) induced mammary tumor in female rats.

MATERIALS AND METHODS

Materials

Paclitaxel, sodium sulfate, sodium metabisulfite, Tween 20, glutaraldehyde (25% in water), 7,12-dimethylbenz[a] anthracene (DMBA), and hyaluronidase enzyme were purchased from Sigma-Aldrich Chemical (St. Louis, MO, USA). The hyaluronic acid sodium salt (from *streptococcus equi* sp.) with M_w 1.5MDa was purchased from Fluka Chemie GmbH (St. Louis, MO, USA). MDA-MB-231 and ZR-75-1 breast cancer cell lines were obtained from American Type Culture Collection ATCC (Manassas, VA, USA). Ki-67 polyclonal antibody was obtained from AbCam (Cambridge, MA). Tetrazolium dye (MTS) assay, phosphate-buffered saline (PBS), MTS CellTiter 96® AqueousONE solution assay, and all other cell culture supplies were purchased from Promega (Madison, WI, USA). All other chemicals and reagents were of analytical grade.

Preparation of Paclitaxel-Loaded Cross-Linked Hyaluronan Nanoparticles

HA was subjected to acidic degradation to produce a low-weight-average molecular weight polymer (20). Briefly, 1% *w*/*v* aqueous solution of HA was degraded in HCl solution (pH 0.5) at 37°C for 24 h. After this time, the pH was adjusted to 7.0, and the solution was subjected to extensive dialysis using Spectra/Por tubing with a molecular cutoff of 3,500 Da. Nanoparticles were prepared using a desolvation method with polymer cross-linking as follows: HA (200 mg) was dissolved in 10 mL of water containing 2% Tween 20. The solution was heated to 40°C with constant stirring at 500 rpm to ensure full mixing. To this solution, 2 mL of a 20% aqueous solution of sodium sulfate was added slowly followed by 1–2 mL of acetone containing 2 or 20 mg of paclitaxel. A second aliquot of sodium sulfate solution (5–6 mL) was added until the solution turned turbid, which indicated the formation of HA aggregates. Approximately 1 mL of distilled water was then added until the solution turned clear. An aqueous solution of glutaraldehyde (25%, 0.6 mL) was added to cross-link the hyaluronic acid (Fig. 1b). Sodium metabisulfite solution (12%, 5 mL) was added 30 min later to stop the cross-linking process. After 2 h, the crude product was purified on a Sephadex G-50 column, and nanoparticle-containing fraction was lyophilized in a freeze-drier over a 48-h period.

High-Pressure Liquid Chromatography Analysis of Paclitaxel

Analyses of PXL concentration was conducted on an Agilent 1100 series chromatographic system (Agilent Technologies, Palo Alto, CA, USA). Chromatographic separation was achieved with a C_{18} *Altima*™ column (4.6 mm ID, 150 mm; 5 μm) from Grace (Grace, MA) protected by a Phenomenex® SecurityGuard™ in-line filter frit (Torrance, CA, USA). The mobile phase consisted of water, methanol, and acetonitrile (25:35:40, *v*/*v*). The mobile phase was filtered through a 0.45-μm filter (Millipore, Bedford, MA, USA) and degassed before use. The high-performance liquid chromatography (HPLC) system was run at ambient temperature with a flow-rate of 1.0 mL/min, and quantitative analysis of peak area under the curve (AUC) was performed at a wavelength of 230 nm with total chromatographic run time of 8 min. The calibration curve for the quantification of paclitaxel was linear over the standard concentration range of paclitaxel at 50–50,000 ng/mL with a correlation coefficient of R^2=0.999. The limit of detection was 50 ng/mL.

Characterizations of PXL-HA NPs

The morphology and size distribution of the PXL-HA NPs were observed using Philips Tecnai 12 Biotwin microscope with an accelerating voltage of 100 kV at the University of Kentucky Medical Center Imaging Facility. A dried nanoparticle sample was dispersed directly into distilled water, and then a copper grid coated with a carbon film was put into the previous suspension several times and left to incubate for 2.0 min at room temperature. After drying and removal of excess fluid, the samples were negatively stained with 2%

uranyl acetate, and the grids were examined and recorded with the transmission electron microscope (TEM) images.

The amount of entrapped paclitaxel in nanoparticles was detected in triplicate by HPLC analysis. Two milligrams of paclitaxel-loaded nanoparticles were dispersed in 0.5 mL of PBS and digested with 0.5 mL of hyaluronidase (1 mg/mL in PBS) in a metabolic shaker at 37°C. After about 1 h, extraction was performed with two volumes of 3 mL of ethyl acetate each. The ethyl acetate layers were pooled, dried under a stream of nitrogen, and reconstituted in 100 μL acetonitrile. The encapsulation efficiency (EE) of paclitaxel in nanoparticles was determined as the mass ratio of the entrapped paclitaxel in nanoparticles to the theoretical amount of paclitaxel used in the preparation.

In Vitro Release of Paclitaxel from HA NPs

A membraneless dissolution method was used for *in vitro* studies (21). PXL-HA NPs (10–20 mg) were incubated in 60 mL of PBS (pH 7.4) at 37°C. To maintain a sink condition, 2 mL of octanol were placed on top of the PBS layer to continuously extract the released paclitaxel from the PBS. At assigned time points, octanol was removed, and a fresh 2 mL of octanol was layered on top of the PBS. Assay for PXL concentration was performed after appropriate dilution in acetonitrile utilizing the HPLC system mentioned earlier.

In Vitro Cytotoxicity of PXL-HA NPs

RPMI 1640 (with 2 mM L-glutamine, 10 mM HEPES, 1 mM sodium pyruvate, 4.5% glucose and 1.5% sodium bicarbonate) and Leibovitz's L15 media were used as culture media and were supplemented with 10% fetal bovine serum (FBS), 50 μg/mL penicillin, and 50 μg/mL streptomycin. In a 96-well plate (Nunclon™), the human breast cancer cell lines MDA-MB-231 and ZR75 were maintained in Leibovitz's L15 and RPMI 1640, respectively. All cells were maintained in an isolated humidified environment with 5% CO_2 at 37°C.

Cytotoxicity of PXL in PBS, PXL-HA NPs, and unloaded HA nanoparticles (blank HA NPs) were determined by measuring the cell growth inhibition using a tetrazolium dye (MTS) assay. MDA-MB-231 and ZR75 cells were seeded in 96-well plates at a density of 5×10^3 cells/well and allowed to attach for 16 h. The following morning, the cells were treated with various concentrations (1 or10 μg/mL) of PXL and HA-PXL NPs in the appropriate complete growth medium. At initial treatment, 24, 48, and 72 h posttreatment, cell proliferation was analyzed using the MTS CellTiter 96® AqueousONE solution assay. Absorbance at 490 nm was measured on an ELx800 Universal microplate BioTek Instruments reader (Winooski, VT, USA). The results are expressed as a percentage of the control-treated cells.

In Vivo Evaluation of Antitumor Efficacy of PXL-HA NPs

The *in vivo* efficacy of the PXL-HA nanoparticles was assessed in female Sprague–Dawley rats. Throughout the experiment, all of the rats were housed under a controlled environment with 12 h light/dark cycles and a temperature of 22±2°C, given a commercial diet with tap water *ad libitum*, and weighed every 7 days. At 6 weeks of age, all rats (n=12) were administered 10 mg of DMBA in 1 mL of sesame oil by intragastric gavage weekly for 2 weeks. Beginning 6 weeks after DMBA administration, animals were palpated once weekly to monitor mammary tumor growth. The survival and the body weight of the rat were recorded. The tumor width (w) and length (l) was recorded with a caliper and tumor size was calculated using the formula ($l\times w^2/2$). All research and testing activities, related to this work, was reviewed and approved by the Institutional Animal Care and Use Committee (IACUC) at the University of Kentucky—Chandler Medical Center, Division of Laboratory Animal Resources (DLAR).

When tumors had grown to approximately 100 mm^3 in the DMBA-treated rats, the animals were randomized into four groups A, B, C, and D (n=3/group). Animals were treated with a single 100 μL intratumor injection of 20 mg paclitaxel/kg body weight PXL-HA NPs, equivalent PXL dose in PBS for groups A and B, respectively. The control groups C and D received a single 100 μL intratumor injection of unloaded HA nanoparticles to assess the polymer safety, and PBS (0.1 M, pH 7.4), respectively. The tumor size was calculated as previously reported. The rats were euthanized when the tumor size reached greater than 15% of body weight. The study was terminated 57 days posttreatment.

The tumors were collected immediately after euthanization or reported mortality. Frozen tumors were fixed in 10% buffered formalin before being embedded in paraffin blocks. Two 4-μm sections were obtained from each tumor. One section was processed for routine hematoxylin and eosin staining for histological assessment. The other section was immunostained using the Ki-67 antibody for assessment of the proliferation index of each tumor (22).

Hematoxylin and eosin-stained sections were microscopically assessed for any evidence of necrosis and degeneration as a reflection of the effect of the drug. Degenerative changes in the form of apoptosis and ballooning degeneration were sought. Immunostained sections were evaluated for the percentage of cells positive for the ki-67 polyclonal antibody. Positive-stained cells showed brown nuclear staining. The percentage of cells was expressed after counting 500 cells in five high-power fields.

Statistical Analysis

The statistical significance was studied using two-way analysis of variance (ANOVA) and two-tailed Student's t tests. Differences were considered to be significant at a level of $P<0.05$.

RESULTS

Preparation and Characterization of PXL-HA NPs

The resulted nanoparticles were spherical in shape with moderate uniformity. Figure 2 shows a transmission electron microscope (TEM) image of HA-PXL NPs. The encapsulation efficiency of PXL into HA nanoparticles was determined as the mass ratio of the entrapped paclitaxel in nanoparticles to the theoretical amount of paclitaxel used in the preparation and was found to be above 90% at the PXL loading utilized in our experiment (Table I). Both of the 1% and 10% loading levels of PXL in the HA nanoparticle formulations

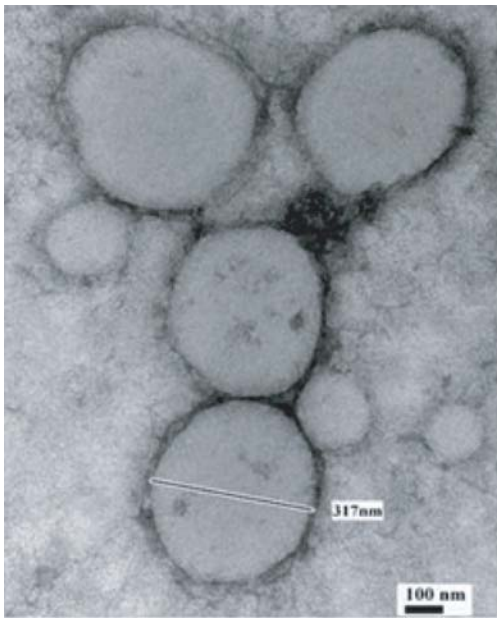

Fig. 2. Transmission electron microscope (TEM) image of paclitaxel-loaded hyaluronan nanoparticles

had shown no statistical significant difference in encapsulation efficiency.

In Vitro Release of Paclitaxel From HA NPs

To evaluate the potential of HA nanoparticles as a drug carrier of PXL, the release behavior of PXL from HA nanoparticles was assessed at 37°C±1 in PBS (pH 7.4). During these experiments, the sink conditions were maintained by regularly replacing the octanol medium. The *in vitro* release profile of PXL-HA (1% drug loading) nanoparticles is shown in Fig. 3. Paclitaxel was released from the drug-loaded HA nanoparticles in a biphasic pattern: a fast release rate in the first 10 h followed by a slow uniform release afterwards. The initial fast drug release can be ascribed to those drugs located on or near the particle surface; while the slow and uniform release could be caused by release of the drugs inside the nanoparticles. In the first 10 h, about 70± 0.4% of the loaded drug was released out of the nanoparticles. The accumulative drug release in 18 h was 90± 1.2%.

In Vitro Cytotoxicity of PXL-HA NPs

As shown in Fig. 4, empty cross-linked HA NPs did not show any toxicity. On the other hand, both the PXL and

Table I. Characterizations of PXL-Loaded HA Nanoparticles

Sample	Theoretically loaded PXL (wt%)	Measured loaded PXL (wt.%)	Encapsulation efficiency (%)	Size (nm)
HA	–	–	–	269±16.2
PXL-HA	1	0.83±0.07	83±7	294±41.2
PXL-HA	10	7.8±0.90	78±9	304.8±28.4

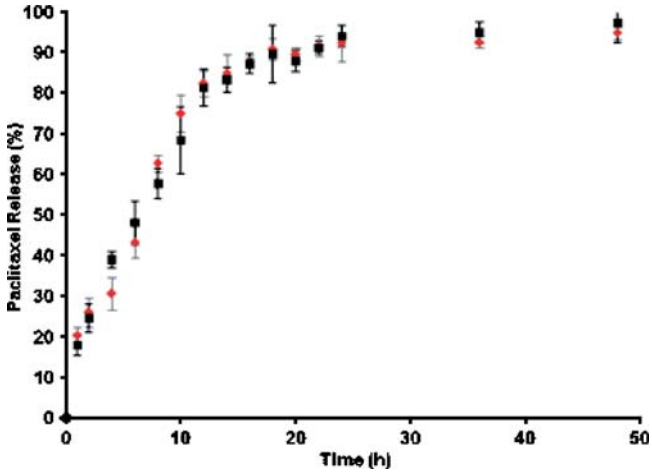

Fig. 3. *In Vitro* accumulated release of PXL from PXL-HA nanoparticles at 1% (*filled diamonds*) and 10% (*filled squares*) PXL loading in PBS at 37.0±0.1°C. Values are means ± SD (n=3)

PXL-HA NPs inhibited growth of the cell lines to relatively similar extents. Nearly less than 75% of the MDA-MB-231 and ZR-75-1 breast cancer cells were viable after a 2-day exposure to PXL and PXL-HA treatment regardless of the dose. Furthermore, two-way ANOVA using a repeated measures design revealed a statistically significant reduction in cell viability at 72 h in the MDA-MB-231 cell line for all

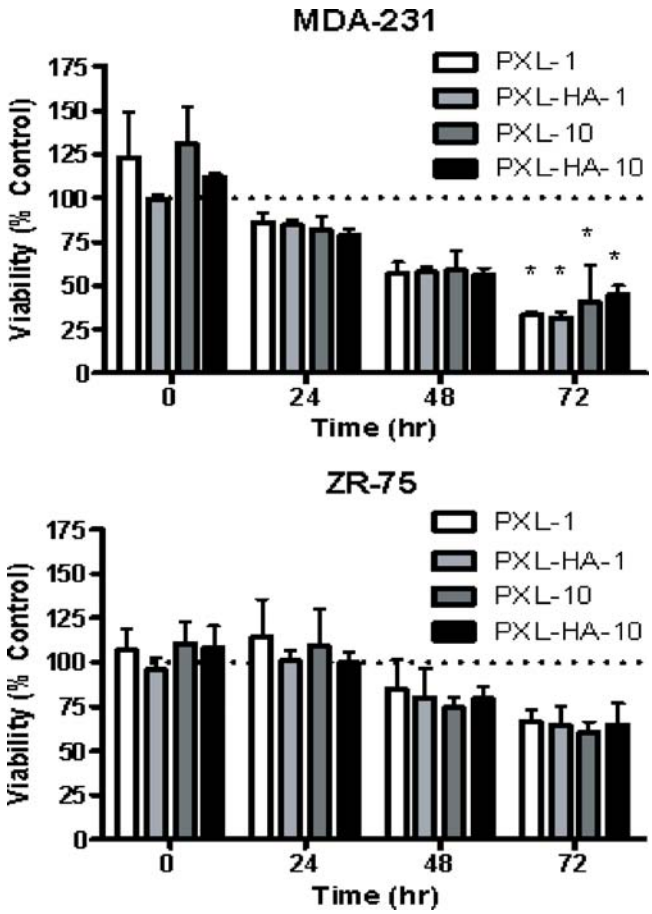

Fig. 4. *In vitro* cytotoxicity study results using MDA-MB-231 (*top*) and ZR-75-1 (*bottom*) human breast cancer cell lines

treatment groups (PXL-1, PXL-HA-1, PXL-10, and PXL-HA-10) relative to the appropriate control treatment. This effect was not observed in the ZR-75 cell line.

These results suggest that HA nanoparticles maintain the pharmacological activity of PXL. Interestingly, however, no advantage on cell growth inhibition was noted in the PXL-HA NPs-treated cells over the free PXL formulation, regardless of CD44 status. This is likely due to the fact that the *in vitro* cell culture model is likely to be incapable of demonstrating an advantage of cell growth inhibition under these conditions, since drug exposure and uptake is not a limiting factor in this model. *In vivo* tumor models would represent a more ideal case to demonstrate such an advantage.

In Vivo Antitumor Effect

There was no significant difference in the initial mean size of the tumor nodules between the PXL-HA NPs and the PXL suspended in PBS groups before treatment. However, the PXL-HA NPs treated group showed effective inhibition of tumor growth in all treated rats. Interestingly, there was one case of complete remission of tumor nodule and two cases of persistent reduction of tumor size that was observed on subsequent days. The mean size of the tumor nodules came close to baseline volume over the 57-day observation period. In the case of the PXL suspended in PBS group, the mean tumor volume increased almost linearly (R^2=0.93) with time to a size that was 4.9-fold larger than the baseline volume at 57 days post-drug administration. The single intratumor injection of PXL-HA NPs therefore produced significant tumor-growth inhibition effect compared to PXL suspended in PBS at the same paclitaxel dose of 20 mg/kg (Fig. 5).

For both the PXL-HA NPs and the PXL suspended in PBS-treated groups, there was no significant weight change in the animals after drug administration, suggesting an absence of significant toxicity associated with the two formulations at the paclitaxel dose of 20 mg/kg (Fig. 6).

Control groups C and D that were treated with a single 100 μL intratumor injection of unloaded HA nanoparticles to assess the polymer safety and PBS exhibited similar tumor

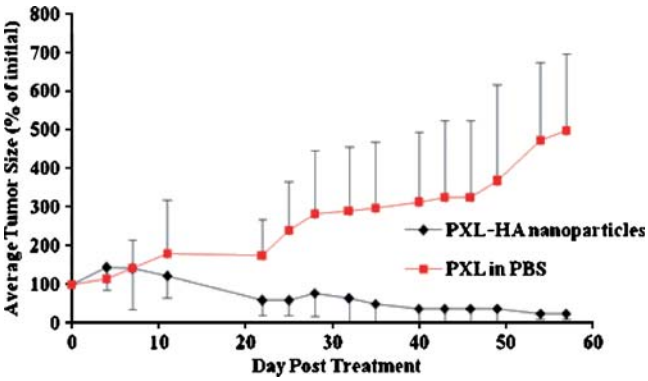

Fig. 5. The change in tumor size in DMBA-treated female SD rats as a function of time after a single intratumor injection with PXL-HA nanoparticles (*filled diamonds*) or PXL in normal saline (*filled squares*) at 20 mg paclitaxel/kg (mean ± SD, n=3; p=0.05)

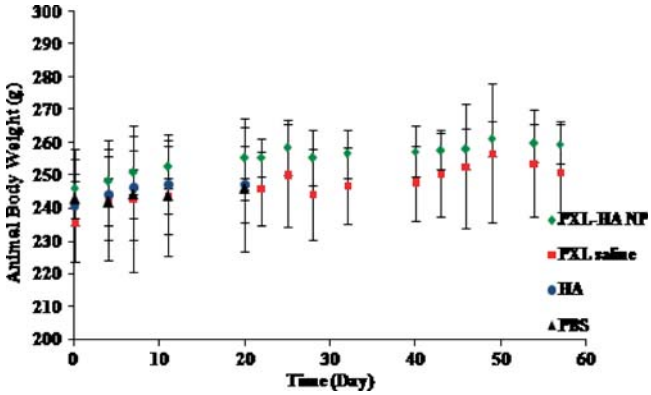

Fig. 6. The change in DMBA-treated animals body weight as a function of time after the rats received intratumor injection of PXL-HA nanoparticles (*filled diamonds*), PXL in normal saline (*filled squares*), HA nanoparticles (*filled circles*) and PBS (*filled triangles*). The intratumor dose of paclitaxel administered was 20 mg/kg. The data are expressed as mean ± SD (n=3)

growth profiles that were characterized by a steady growth of the tumor nodule with time (Fig. 5). The changes in tumor size at day 10 were comparable for both control groups. In addition, the rate of tumor growth in these vehicle-treated groups was comparable to that seen in rats treated with PXL suspended in PBS, suggesting that PXL suspended in PBS at a paclitaxel dose of 20 mg/kg did not effectively inhibit the growth of DMBA-induced tumor in rats. Within 2–3 weeks, the control groups which were treated with HA or PBS had an increase in tumor size up to ten times the initial tumor size before treatment. Two rats from the PBS-treated rats were euthanized after 2 weeks because their tumor size reached greater than 15% of their body weight. The rest of rats in these groups could not survive after 3 weeks, and their tumors were collected after reporting their death.

Histopathology analysis of collected tumors illustrated that tumors treated with intratumor injection of free PXL showed no significant necrosis or degenerative changes. Ki-67 labeling indices in these tumors were 5% to 10% (Fig. 7a b). On the other hand, tumors treated with intratumor injection of PXL-HA NPs showed areas of degeneration in the form of apoptosis and vacuolization with areas of necrosis. The ki-67 labeling indices in both tumors was 0% indicating no growth (Fig. 8a b)

DISCUSSION

Our interest in HA was prompted by its potential as a drug carrier in cancer chemotherapy. Several reviews have previously discussed the advantages of HA as a drug carrier and a targeting ligand for cancer, as well as other pathologies (23–28). Direct intratumoral delivery systems have significant potential advantages due to providing higher drug concentration at the target site compared with systemic routes and circumvention of the various physiological barriers to tumor drug delivery including the high interstitial pressure common to most solid tumors (29). The feasibility of directly injecting tumors has been greatly advanced recently by the utilization of nanoparticle pharmaceutical technology, which permit the enhanced delivery of drugs to the cytoplasm of the cancer cells (30).

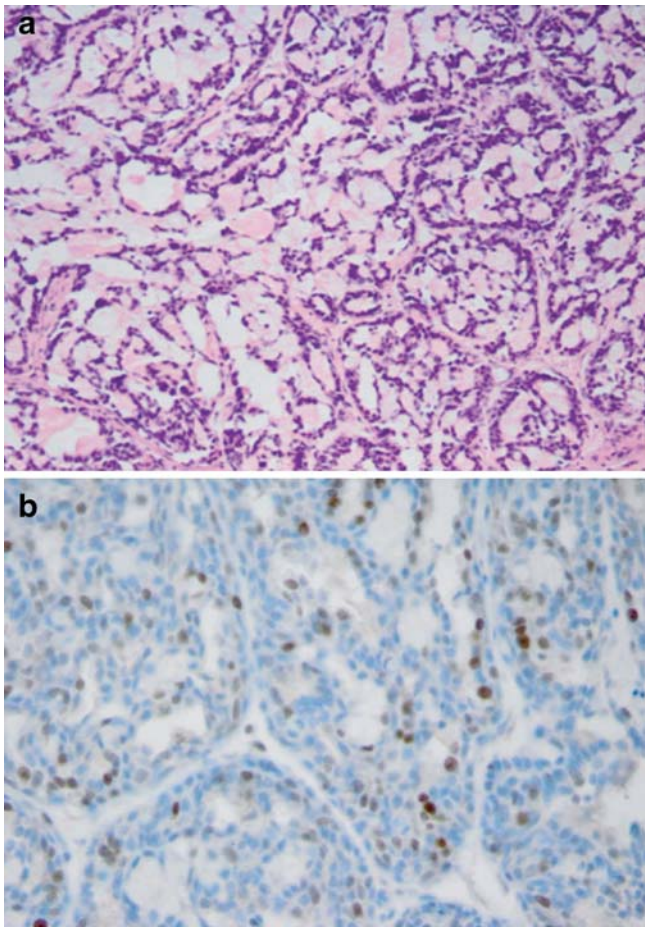

Fig. 7. **a** HE (hematoxylin and cosin) stains of tumor harvested from a rat treated with a single intratumor injection of PXL in PBS (20 mg/kg) at day 57 posttreatment. The tumor tissue shows a viable adenocarcinoma. **b** Tumor harvested from a rat treated with a single intratumor injection of PXL in PBS (20 mg/kg) at day 57 posttreatment showing a Ki-67 labeling index of 10% (immunoperoxidase ×200)

Cross-linked hyaluronan nanoparticles are nano-sized and can be attractive delivery candidates for a variety of biomedical applications. Furthermore, the biocompatibility of the HA nanoparticles, the high affinity toward cancer cells, and the suitable physicochemical properties of these HA nanoparticles make it as a nano-drug delivery system being capable of selectively inhibiting cancer cells of solid tumor and metastatic tumor. In the current study, the developed PXL-HA NPs particle size and the EE were not significantly influenced by the PXL-loading levels utilized in this study. This suggests that PXL molecules are entrapped into the hydrophobic HA inner cores and the entrapped PXL molecules at the loading levels utilized here did not alter significantly the average diameter of the HA nanoparticles.

For a drug to be released from nanoparticles, the release medium must diffuse into the particle and dissolve the entrapped drug, which then diffuses out of the nanoparticle (31). The HA nanoparticles released paclitaxel *in vitro* almost completely over a 50-h period. The cumulative release of the drug did not show any significant difference in PXL release rate between the 1% and 10% PXL loaded nanoparticles in PBS at 37.0±0.1°C with almost 90% released in 2 days period. This could be attributed mainly to two properties of HA nanoparticles that are favorable for drug release. First, compared with microparticles, the small, submicron size of the nanoparticles decrease the effective diameter for the release medium to reach the drug and for outward drug diffusion. Second, the hydrophilicity of HA polymer enhances fluid uptake, which would result in enhanced drug release.

As shown in Fig. 3, paclitaxel was released from the drug-loaded HA NPs in a biphasic pattern: a fast release rate in the first 24 h followed by a slow uniform release afterwards. The initial fast drug release can be ascribed to those drugs located on or near the particles surface; while the slow and uniform release could be caused by diffusion of the drugs inside the nanoparticles.

In order to determine if the paclitaxel-loaded cross-linked hyaluronan nanoparticles retained pharmacologic activity *in vitro*, an MTS assay was performed to compare cell proliferation of two breast cancer cell lines, MDA-231 and ZR-75, in the presence of free paclitaxel or PXL-HA nanoparticles. To ensure that the cytotoxicity was caused by PXL itself and not by the polymer, cells were also incubated

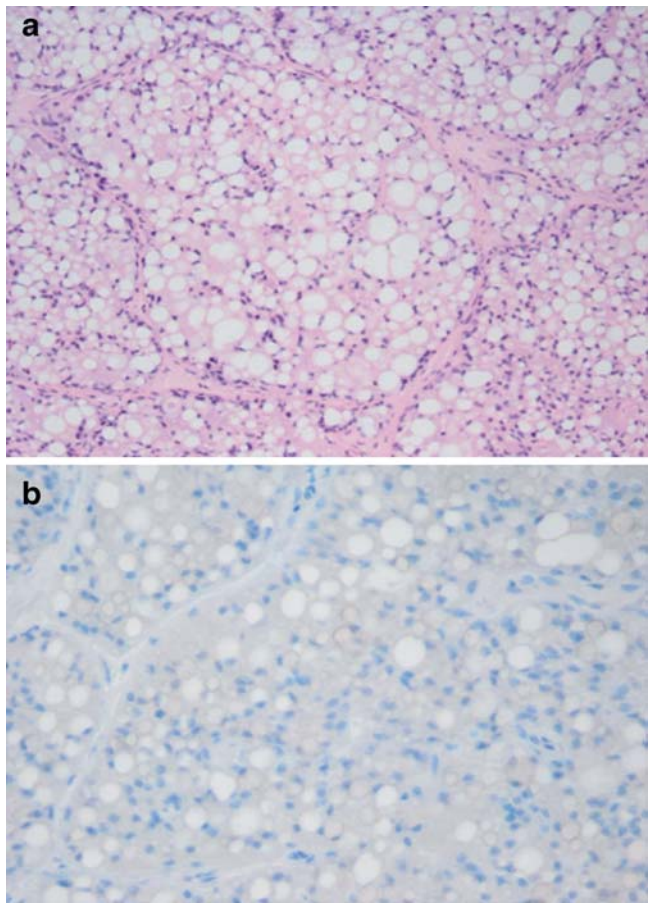

Fig. 8. **a** HE (hematoxylin and cosin) stains of tumor harvested from a rat treated with a single intratumor injection of PXL-HA nanoparticles (20 mg/kg) at day 57 posttreatment. The tumor tissue shows degenerative and necrotic changes in the form of cytoplasmic vacuolization, fatty change, and apoptosis. **b** Tumor harvested from a rat treated with a single intratumor of PXL-HA nanoparticles (20 mg/kg) at day 57 treatment showing a Ki-67 labeling index of 0% (immunoperoxidase ×200)

with empty cross-linked HA nanoparticles. HA exhibits a number of properties of a successful drug carrier. This water soluble, nonimmunogenic polysaccharide has multiple functional groups available for chemical conjugation (24,25). Furthermore, since it is the major CD44 ligand, HA can be used to target cells on which CD44 is expressed (26). In the current study, we utilized the HA polymer locally to enhance the drug delivery to the cancer cells rather than to target the cells after systemic delivery. The MDA-MB-231 and ZR-75-1 cells are both human breast epithelial cancer cell lines. However, the MDA-MB-231 cells express positive CD44 receptor on their surface, while ZR-75-1 cells are deficient in the receptor (32,33). The *in vitro* cytotoxicity studies demonstrated that the placebo HA NPs (without paclitaxel encapsulated) was nontoxic by MTS assay at the studied nanoparticle concentration levels, which implies that the polymer is biocompatible. Furthermore, the drug-loaded HA nanoparticles maintained the pharmacological activity of PXL. Interestingly, however, no advantage on cell growth inhibition was noted in the PXL-HA nanoparticle-treated cells over the free PXL formulation, regardless of CD44 status. This is likely due to the fact that, generally, PXL enters the tumor cell by diffusion and most nanoparticles by endocytosis. However, due to the larger NP size in the current study (>300 nm) and the drug-release kinetics at pH 7.4, PXL is released most likely from the HA-PXL NP at the extracellular matrix and then enters the cell afterwards by diffusion. On the other hand, in the *in vivo* scenario, HA NPs are most likely acting as a shield that keeps the drug for a more prolonged time intratumorally and, therefore, enhancing the therapeutic effect. Furthermore, the *in vitro* cell culture model is likely to be incapable of demonstrating an advantage of cell growth inhibition under these conditions, since drug exposure and uptake is not a limiting factor in this model. *In vivo* tumor models would represent a more ideal case to demonstrate such an advantage.

Solid tumors have several potential barriers to drug delivery that may limit drug penetration, such as alterations in the distribution of blood vessels, blood flow, and interstitial pressure (34,35). Therefore, high systemic levels of the cytotoxic drug often cause a related systemic toxicity without reaching the tumor at effective concentrations. The focus for this current study was to deliver the cytotoxic agent locally. The PXL-HA NPs formulation is injectable through a 23-gauge needle to the tumor tissue, and it was examined in female Sprague–Dawley rats bearing DMBA-induced tumor. After treatment, it was found that the average tumor volume as a function of time was significantly less for the tumor-bearing rats injected with PXL-HA NPs compared to the free PXL intratumor injection. There was no significant difference in the initial mean size of the tumor nodules between the PXL-HA NPs and the PXL suspended in PBS groups before treatment. However, the PXL-HA NPs treated group showed effective inhibition of tumor growth in all treated rats. There was even one case of complete remission of tumor nodule and two cases of persistent reduction of tumor size that was observed on subsequent days. The mean size of the tumor nodules remained at close to baseline volume or even below through shrinking over the next 57 days. In the case of the PXL suspended in PBS group, the mean tumor volume increased almost linearly with time to a size that was 4.9-fold larger than the baseline volume at 57 days post-drug administration. This was in agreement with the histopathology analysis of the tumor tissue collected from both treatment groups. Tumors collected from rats treated with intratumor injection of free PXL showed a proliferation index reflecting moderate proliferation, while the tumors collected from rats treated with intratumor injection of PXL-HA NPs had a Ki-67 proliferative index indicating no growth in such cells suggesting that they were exposed to an effective cytotoxic treatment. It is known that the Ki-67 is an antigen expressed in cells that are not in the G0 phase, but in G1, G2, S, and M phases and that tumors with a high ki-67 proliferative index are rapidly growing and aggressive (22). Therefore, the single intratumor injection of PXL-HA NPs produced significant tumor-growth inhibition effect compared to free PXL suspended in PBS at the same paclitaxel dose of 20 mg/kg. Although we did not see any mortality following single-dose intratumor administration of free PXL or PXL-HA NPs at 20 mg/kg, the tumor volume results clearly show that the PXL-HA NPs formulation was significantly efficacious in decreasing the tumor size and propagation relative to free PXL or control treatment. Furthermore, weight change of an animal after drug administration is often used to evaluate the toxicity of the drug treatment (36). For both the PXL-HA NPs and the PXL suspended in PBS-treated groups, there was no significant weight change in the animals after drug administration, suggesting an absence of significant toxicity associated with the two formulations at the paclitaxel dose of 20 mg/kg.

CONCLUSION

We have developed cross-linked HA nanoparticles loaded with paclitaxel. The resulting nanoparticles had cytotoxicity similar to that of free paclitaxel *in vitro* with superior antitumor efficacy *in vivo* when administered with intratumor injection for the treatment of DMBA-induced mammary tumor in rats. Histological studies proved the existence of the necrotic process caused by the cytotoxic drug. Thus, the direct administration of PXL-HA NPs at the tumor sites could be a promising treatment modality for solid tumors, and further testing is warranted to evaluate the formulation clinically.

ACKNOWLEDGMENT

This research was supported by grant no. 85-001-19-IRG to AMA from the American Cancer Society.

REFERENCES

1. Deurloo MJ, Kop W, van Tellingen O, Bartelink H, Begg AC. Intratumoural administration of cisplatin in slow-release devices: II. Pharmacokinetics and intratumoural distribution. Cancer Chemother Pharmacol 1991;27 5:347–53.
2. Aigner KR. Intra-arterial infusion: overview and novel approaches. Semin Surg Oncol 1998;14 3:248–53.
3. Lee JD, Yang WI, Lee MG. Effective local control of malignant melanoma by intratumoural injection of a beta-emitting radionuclide. Eur J Nucl Med Mol Imaging 2002;29 2:221–30.
4. Zhang X, Jackson JK, Wong W. Development of biodegradable polymeric paste formulations for taxol: an *in vitro* and *in vivo* study. Inter J Pharm 1996;137 2:199–208.

5. Dhanikula AB, Panchagnula R. Development and characterization of biodegradable chitosan films for local delivery of paclitaxel. AAPS J 2004;6 3:e 27.
6. Ho EA, Vassileva V, Allen C, Piquette-Miller M. *In vitro* and *in vivo* characterization of a novel biocompatible polymer–lipid implants system for the sustained delivery of paclitaxel. J Cont Rel 2005;104 1:181–91.
7. Ramaswamy M, Zhang X, Burt HM, Wasan KM. Human plasma distribution of free paclitaxel and paclitaxel associated with diblock copolymers. J Pharm Sci 1997;86 4:460–4.
8. Luo Y, Prestwich GD. Synthesis and selective cytotoxicity of a hyaluronic acid–antitumor bioconjugate. Bioconjug Chem 1999;10 5:755–63.
9. Lokeshwar VB, Selzer MG. Differences in hyaluronic acid-mediated functions and signaling in arterial, microvessel, and vein-derived human endothelial cells. J Biol Chem 2000;275 36:27641–9.
10. Obara K, Ishihara M, Ozeki Y. Controlled release of paclitaxel from photocrosslinked chitosan hydrogels and its subsequent effect on subcutaneous tumor growth in mice. J Control Release 2005;110 1:79–89.
11. Hardingham T, Fosang A. Proteoglycans: many forms and many functions. FASEB J 1992;6 3:861–70.
12. Hoare K, Savani RC, Wang C, Yang B, Turley EA. Identification of hyaluronan binding proteins using a biotinylated hyaluronan probe. Connect Tissue Res 1993;30 2:117–26.
13. Turley EA, Belch AJ, Poppema AJ, Pilarski LM. Expression and function of a receptor for hyaluronan-mediated motility on normal and malignant lymphocytes-B. Blood 1993;81 2:446–53.
14. Vazquez E, Dewitt DM, Hammond PT, Lynn DM. Construction of hydrolytically-degradable thin films via layer-by-layer deposition of degradable polyelectrolytes. J Am Chem Soc 2002;124 47:13992–3.
15. Benkirane-Jessel N, Schwinte P, Falvey P. Build-up of polypeptide multilayer coatings with anti-inflammatory properties based on the embedding of piroxicam–cyclodextrin complexes. Adv Funct Mater 2004;14 2:174–82.
16. Guyomard A, Nysten B, Muller G, Glinel K. Loading and release of small hydrophobic molecules in multilayer films based on amphiphilic polysaccharides. Langmuir 2006;22 5:2281–7.
17. Berg MC, Zhai L, Cohen RE, Rubner MF. Controlled drug release from porous polyelectrolyte multilayers. Biomacromolecules 2006;7 1:357–64.
18. Massey PJ, Chen TT, Caudle MR. Biphasic steroidogenic effects of taxol and cremophor EL. Endocrine 1994;2 10:891–7.
19. Cella D, Peterman A, Hudgens S, Webster K, Socinski MA. Measuring the side effects of taxane therapy in oncology: the functional assessment of cancer therapy-taxane (FACT-taxane). Cancer 2003;98 4:822–31.
20. Shu XZ, Liu Y, Palumbo FS, Prestwich GD. Disulfide-crosslinked hyaluronan-gelatin hydrogel films: a covalent mimic of the extracellular matrix for *in vitro* cell growth. Biomaterials 2003;24 21:3825–34.
21. Barichello JM, Morishita M, Takayama K, Nagai T. Encapsulation of hydrophilic and lipophilic drugs in PLGA nanoparticles by the nanoprecipitation method. Drug Dev Ind Pharm 1999;25 4:471–6.
22. Isik Gonul I, Akyurek N, Dursun A, Kupeli B. Relationship of Ki67, TP53, MDM-2 and BCL-2 expressions with WHO 1973 and WHO/ISUP grades, tumor category and overall patient survival in urothelial tumors of the bladder. Pathol Res Pract 2008;204 10:707–17.
23. Pouyani T, Prestwich GD. Functionalized derivatives of hyaluronic acid oligosaccharides: drug carriers and novel biomaterials. Bioconjug Chem 1994;5 4:339–47.
24. Prestwich GD, Marecak DM, Marecek JF, Vercruysse KP, Ziebell MR. Controlled chemical modification of hyaluronic acid: synthesis, applications, and biodegradation of hydrazide derivatives. J Controlled Release 1998;53 1–3:93–103.
25. Vercruysse KP, Prestwich GD. Hyaluronate derivatives in drug delivery. Crit Rev Ther 1998;15 5:513–55.
26. Jaracz S, Chen J, Kuznetsova LV, Ojima I. Recent advances in tumor-targeting anticancer drug conjugates. Bioorg Med Chem 2005;13 17:5043–54.
27. Liao YH, Jones SA, Forbes B, Martin GP, Brown MB. Hyaluronan: pharmaceutical characterization and drug delivery. Drug Delivery 2005;12 6:327–42.
28. Yadav AK, Mishra P, Agrawal GP. An insight on hyaluronic acid in drug targeting and drug delivery. J Drug Targ 2008;16:91–107.
29. Thorpe PE. Vascular targeting agents as cancer therapeutics. Clin Cancer Res 2004;10:415–27.
30. Zamboni WC. Liposomal, nanoparticle, and conjugated formulations of anticancer agents. Clin Cancer Res 2005;11 23:8230–4.
31. Alonso MJ, Cohen S, Park TG, Gupta RK, Siber GR, Langer R. Determinants of release rate of tetanus vaccine from polyester microspheres. Pharm Res 1993;10 7:945–53.
32. Culty M, O'Mara TE, Underhill CB, Yeager H Jr, Swartz RP. Hyaluronan receptor (CD44) expression and function in human peripheral blood monocytes and alveolar macrophages. J Leukoc Biol 1994;56 5:605–11.
33. Herrera-Gayol A, Jothy S. Effects of hyaluronan on the invasive properties of human breast cancer cells *in vitro*. Int J Exp Pathol 2001;82 3:193–200.
34. Jain RK. Delivery of molecular medicine to solid tumors. Science 1996;271 5252:1079–80.
35. Curnis F, Sacchi A, Corti A. Improving chemotherapeutic drug penetration in tumors by vascular targeting and barrier alteration. J Clin Inv 2002;110 4:475–82.
36. Harper E, Dang W, Lapidus RG, Garver RI. Enhanced efficacy of a novel controlled release paclitaxel formulation (PACLIMER delivery system) for local–regional therapy of lung cancer tumor nodules in mice. Clin Cancer Res 1999;5 12:4242–8.